Proceedings of 6th ICCHMT
May 18–21, 2009, Guangzhou, CHINA
243

COMPUTATIONAL ANALYSIS OF TURBULENT SWIRLING FLOW IN WATER MODEL OF A GAS TURBINE COMBUSTOR

A. C. Benim*†, M. Cagna‡, F. Joos+, A. Nahavandi†, A. Wiedermann‡
†Department of Mechanical and Process Engineering, Duesseldorf University of Applied Sciences, Josef-Gockeln-Str. 9, D-40474 Duesseldorf, Germany
‡MAN Turbo, R&D Gas Turbines, Oberhausen, Germany
+Laboratory of Turbomachinery, Helmut Schmidt University, Hamburg, Germany
*Corresponding author: Fax: +49 211 43 51 409 Email: alicemal.benim@fh-duesseldorf.de

ABSTRACT
Turbulent swirling flow in water model of a gas turbine combustor is computationally investigated. As the basic modeling strategy, a three-dimensional unsteady RANS approach is applied, employing a differential Reynolds stress turbulence model. A highly unsteady and three-dimensional flow structure, exhibiting vortex breakdown and a precessing vortex core is observed. For a better understanding and demonstrating the influence of different modeling approaches, computations are carried out for different modeling parameters, comparing their results. These include the solution domain definition, turbulence modeling, the time-step size and the time-averaging period.

INTRODUCTION
Swirling flows have been the subject of intensive experimental, analytical and numerical investigation over many years [1-2]. The application of swirling flows in industrial gas turbine combustors is of particular interest to the current work. In such systems, a high degree of swirl is imparted to the main combustion air in order to induce a vortex breakdown reverse flow zone along the axis of the combustor, to ensure flame stability and high combustion efficiency. Prediction of such flows is, therefore, of paramount importance to combustor design.

It is known that certain Reynolds stresses are strongly modified due to the action of flow curvature and pressure gradient in swirling flows. Therefore, much of the computational work dealing with swirling flows were based on Reynolds Stress Models (RSM) [3,4]. Nevertheless, it is also observed [5] that RSM based procedures, applied within a RANS formulation may also produce inferior results. This is expected to be caused by the low frequency transient motion of coherent structures, which can occur in swirling flows, and can not adequately be taken into account by a RANS turbulence model. This has led, at the first stage, to the application of RSM within a URANS formulation, which had to be applied in three-dimensions, since the flow transience is intimately related with three-dimensionality (3D URANS RSM) and, to LES (Large Eddy Simulations), where, encouraging results have indeed been obtained by these models [6]. The analysis has been extended to different flow configurations [7,8], where a cascade of modelling procedures including 3D URANS RSM, LES and DES (Detached Eddy Simulations) have been assessed.

In the authors' previous work [6-8], Reynolds numbers of the considered flows have been rather low (4000-7000), where the possible role of transitional effects had to be addressed. In the present investigation, the turbulent swirling flow in a water test rig is investigated, which operates at a much higher Reynolds number of Re=55000. This Reynolds number resembles the real combustor conditions much more realistically. This is one of the distinguishing features of the present study. Furthermore, the influence of different modeling parameters on the numerical accuracy, such as the geometry of the solution domain, turbulence modeling, the time-step size, and the time-averaging period are investigated.

MODELLING

The computational analysis is performed based on the general purpose CFD code ANSYS-CFX [9]. As the basic modeling strategy, a 3D URANS-RSM procedure is applied. For comparison, the Shear Stress Transport (SST) model [9] is also applied within the 3D URANS formulation for assessing the performance of RSM vs. SST. The RSM and SST models are also applied within a 2D-axisymmetric RANS formulation, and the results are compared with 3D URANS ones. The near-wall turbulence is modeled by the wall-functions approach [9]. For the spatial discretization of the momentum equations, a high resolution scheme [9] is applied, whereas the upwind scheme is used for the turbulence equations. For the temporal discretization, a second-order backward Euler scheme is employed. In the main computations (the so-called "base case"), the time-step size is chosen in such a way that the cell Courant number while sufficiently resolving important physical time scales such as the eddy turnover time.

GEOMETRY, BOUNDARY CONDITIONS

Geometry of the water test rig is shown in Figure 1a. The swirler is on the top. The direction extending from the swirler downwards will be referred to as the axial direction (x). The water flows into the domain upwards through the annular inlet. As it then flows radially inwards through the swirler, swirl is imparted to the fluid. Following the swirler, the flow is channeled into the axial direction (downwards), and after flowing through a short throat section and a short section with diverging area, reaches the main combustor domain, and finally, the outlet region with a sudden area expansion with a sidewards outlet pipe. The flow rate is such that the Reynolds number based on the bulk velocity and diameter of the main combustor body is 55000. At the inlet a uniform velocity profile is prescribed. Turbulence variables are derived assuming a turbulence intensity of 5% and an isotropic turbulence. The turbulence energy dissipation rate is estimated by assuming a ratio of 10 between the turbulent and molecular viscosity. At the outlet, the static pressure is prescribed, with a zero-gradient boundary conditions for remaining variables (Figure 1a). Computations are also carried out for a solution domain without the swirler, as shown in Figure 1b, right, where the inlet boundary is placed on the cylindrical surface just downstream the swirler guide vanes. The inlet boundary conditions on that surface are obtained by circumferential averaging of

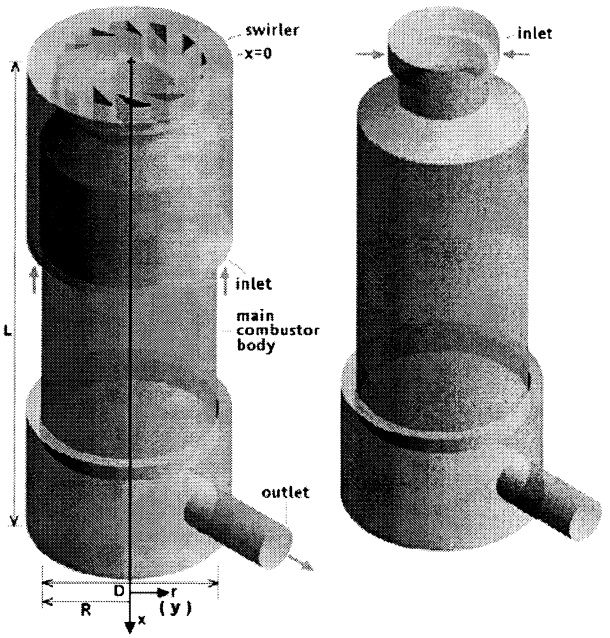

(a) (b)

Figure 1
Solution domain:
a: with swirler, b: without swirler

the time-averaged distributions at that position, which stem from the computations with swirler (Figure 1a). Thus, they are functions of the axial coordinate (x) (Figure 1b). In 2D-axisymmetric computations, the swirler body could not be modelled, of course. So, the inlet boundary of the 2D-axisymmetric computations corresponds to the inlet boundary of the 3D computations without swirler (Figure 1b). In the 2D-axisymmetric modeling, the outlet pipe (Figure 1) is approximated by an radially extending axisymmetric tiny slit with the same cross-sectional area as the outlet pipe (Figure 1).

GRIDS

A formal grid dependency study in 3D is not performed. Indications of the required grid fineness are obtained through preliminary 2D-axisymmetric RANS computations, while avoiding too large expansions, distortions and aspect ratios of the cells in generating the 3D grid. The grid generation is also guided by the idea of obtaining optimal near-wall y^+ values for the wall-functions approach. The resulting average y^+ values are about 60 for the swirler channels and 140 for the combustor domain, which can be considered to be quite favorable. The grid is generated using a conformal block-structured strategy, using hexahedral cells. Figure 2 shows two

sections of the 3D grid for the case with swirler, which consists of about 1,800,000 nodes. The grid for the case without swirler (or for the 2D-axisymmetric case) is analogous to the one with swirler for the corresponding geometry.

COMPUTATIONAL DETAILS

Based on the bulk velocity (U) and the diameter (D) of the main combustor body, an integral time scale (T_I) can be defined. In the 3D URANS analysis, for each case, the unsteady computations are carried out for an initial period of time that is approximately equal to the integral time scale (T_I), without time-averaging. This is done for preventing a possible pollution of the time-averaged values by the initial fields that are not necessarily physical. After this initial period, the time-averaging is started, and carried out for a time-averaging period of T. Further computational details will be given below.

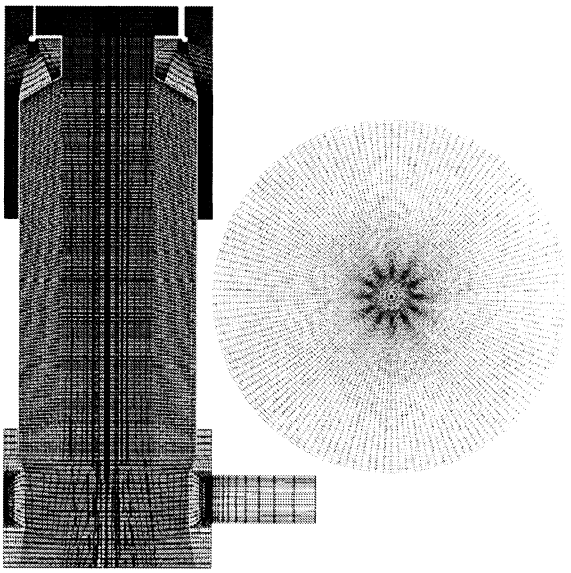

(a) (b)

Figure 2
Sections of 3D grid with swirler:
a: longitudinal section, b: lateral section

RESULTS

Main flow field characteristics: Some important characteristics of the predicted flow field are discussed in the present section. The underlying computations are those of the "**base case**", which is defined as: 3D URANS RSM modelling, the swirler is included in the solution domain (Figure 1a), $\Delta t = T_I / 8000$, $T = 12\ T_I$.

Figure 3 shows the velocity vectors for a time step, and in time-average, in the near-field of the swirler, in a longitudinal section through burner centerline. The distribution for an instant of time reveals the strongly three-dimensional unsteady nature of the flow. The time-averaged vector field is quite symmetric and smooth. The typical characteristics of high swirl number flows, i.e. the vortex breakdown and the associated inner recirculation zone that extends far upstream inside the burner can be observed. Due to the quite rapid expansion of the cross-sectional area after the throat section (that follows the swirler sections), external recirculation zones are additionally formed.

Figure 4 is aimed to illustrate the shape of the time-averaged inner recirculation zone. In this figure, the forward flow region (positive x-velocity, downwards) is colored by blue and the backward flow region (negative x-velocity, upwards) by red. One can see

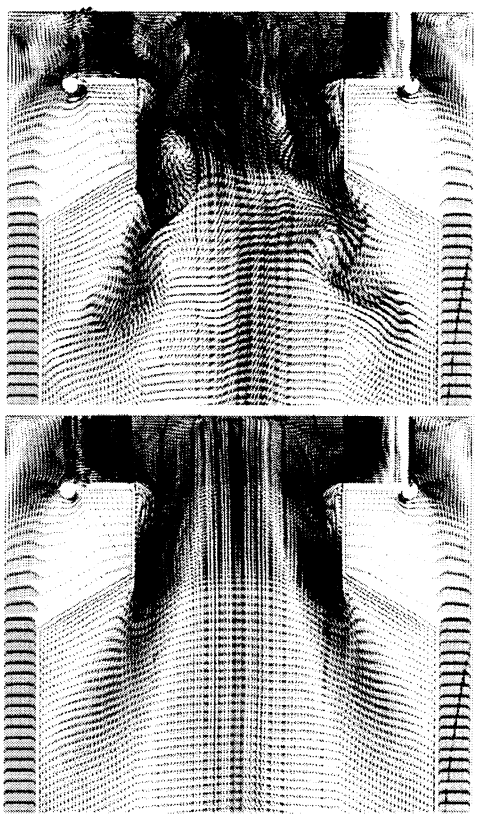

(a)

(b)

Figure 3
Velocity vectors in a longitudinal section:
a: at a time step, b: time-averaged

One can see that even for $T/T_I = 12$, a perfectly steady-state time-averaged result can not be claimed. Nevertheless, the difference between the two higher T values is quite small (approx 2%). Variations of the time-averaged axial velocity along the combustor axis, predicted for different T values are displayed in Figure 7. The curves for $T/T_I = 7$, 12 are practically identical. Increasing deviations are observed for decreasing T ($T/T_I = 4.4$, 1.6). A fairly steady-state time-averaged solution seems to be obtained for $T/T_I \geq 7$.

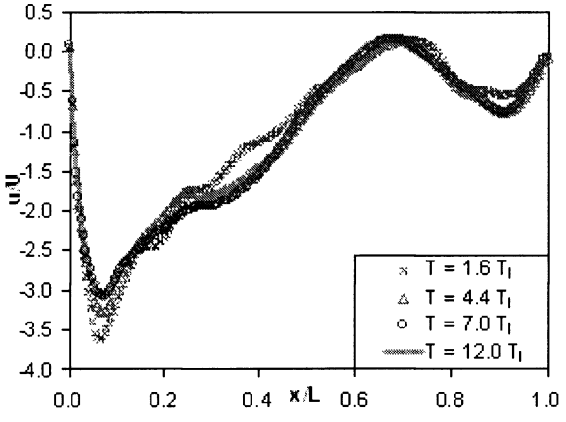

Figure 7
Time-averaged axial velocity profile along combustor axis for different T

Influence of time-step size: In this section, the influence of the time-step size is investigated. These computations are performed for the configuration without the swirler (Figure 1b). The 3D URANS RSM modeling is used in all computations. The time-averaging period is commonly $T = 7\ T_I$. The time-step size of the "base case" has been $\Delta t_B = T_I / 8000$, which results in maximum cell Courant numbers slightly below unity. Figure 8 compares the predicted distributions of the time-averaged axial (u) and circumferential (w) velocity components for different values of Δt, namely for $\Delta t = \Delta t_B$, $\Delta t = 2\ \Delta t_B$, $\Delta t = 4\ \Delta t_B$, along a traversal line at x/L=0.2. A similar comparison for x/L=0.4 is provided in Figure 9. It is interesting to see that the results are practically the same. This implies that the time-step sizes that result in maximum cell Courant number smaller than 4 provide sufficient accuracy for the time-averaged quantities. A further doubling of the time-step size

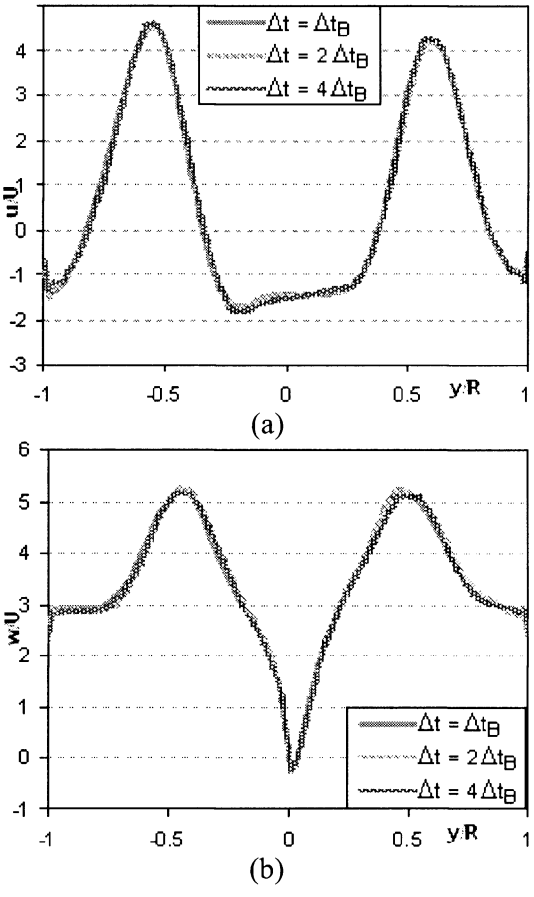

Figure 8
Time-averaged velocity profiles for different Δt along a line at x/L=0.2:
a: axial velocity, b: circumferential velocity

beyond $\Delta t = 4\ \Delta t_B$, i.e. to $\Delta t = 8\ \Delta t_B$, has but led to divergence.

Influence of inlet boundary definition: The configurations with (Figure 1a) and without (Figure 1b) swirler are compared. In both computations, 3D URANS RSM modeling and the parameters: $T = 7\ T_I$, $\Delta t = T_I / 8000$ are employed. Predicted variations of time-averaged axial (u) and circumferential (w) velocities along a traversal line at x/L=0.2 with and without swirler are shown in Figure 10. A similar comparison is provided in Figure 11 for x/L=0.4. At x/L = 0.2, the omission of the swirler leads to an under-prediction of the backflow velocities of the inner recirculation

zone (Figure 10a). The circumferential velocities are not that strongly influenced at the same position

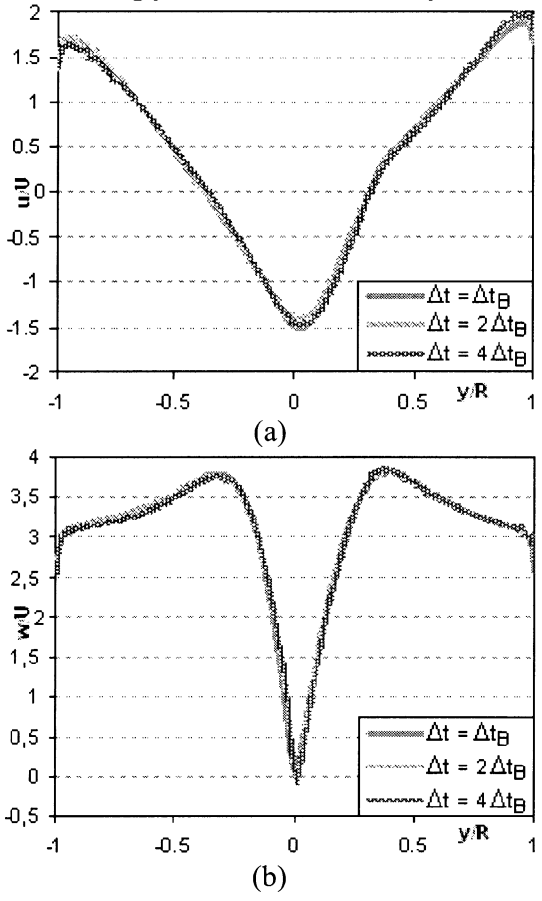

Figure 9
Time-averaged velocity profiles for different Δt along a line at x/L=0.4:
a: axial velocity, b: circumferential velocity

(Figure 10b). At the further downstream position of x/L = 0.4, the both velocity components don't show substantial differences between the cases with and without swirler (Figure 11).

Influence of turbulence modeling: This comparison is performed for the geometry without swirler (Figure 1b). The following parameters hold: $\Delta t = T_I / 8000$, $T = 7\ T_I$. Within the framework of 3D URANS modeling the Reynolds Stress Model (RSM) and the Shear Stress Transport model (SST) are compared. In addition, 2D axi-symmetric RANS computations using RSM and SST are also performed. The 2D RANS SST model has lead to converged results, although the 3D RANS SST model captures flow unsteadiness. The artificial suppression of flow three-dimensionality (that is

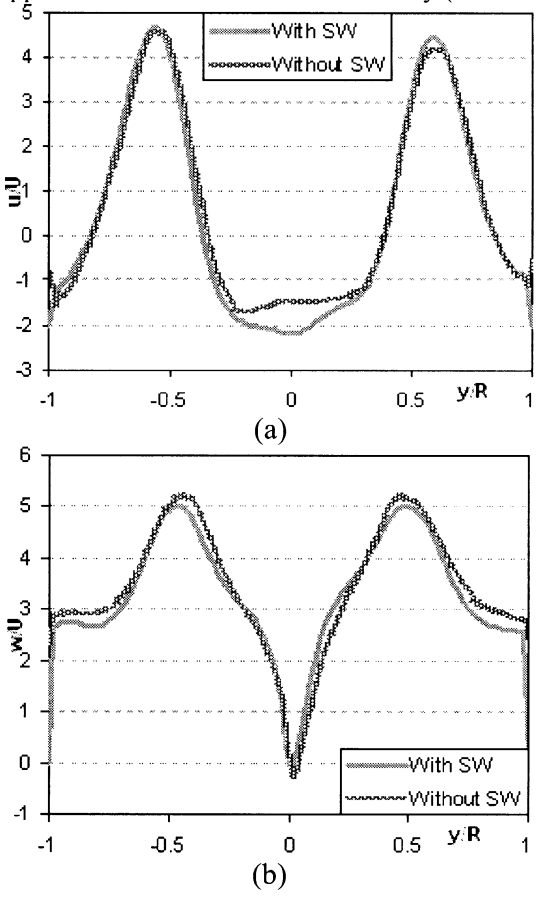

Figure 10
Time-averaged velocity profiles with and without swirler along a line at x/L=0.2:
a: axial velocity, b: circumferential velocity

intimately related with flow unsteadiness) in the 2D modeling may be the reason for this behavior. The 2D RANS RSM computation has not lead to converged results, indicating that RSM captures some flow unsteadiness even within a 2D formulation, for this case. Thus, for the 2D application of RSM, unsteady computations are performed (2D URANS RSM) that are presented in the following figures.

Figure 12 compares the predicted distributions of the time-averaged axial (u) and circumferential (w) velocity, along a traversal line at x/L=0.2, for different turbulence modeling approaches. A similar comparison for x/L=0.4 is provided in Figure 13. Based on the profiles of time-averaged axial

velocity at x/D=0.2, one can see that 3D URANS SST over- predicts the size and intensity of

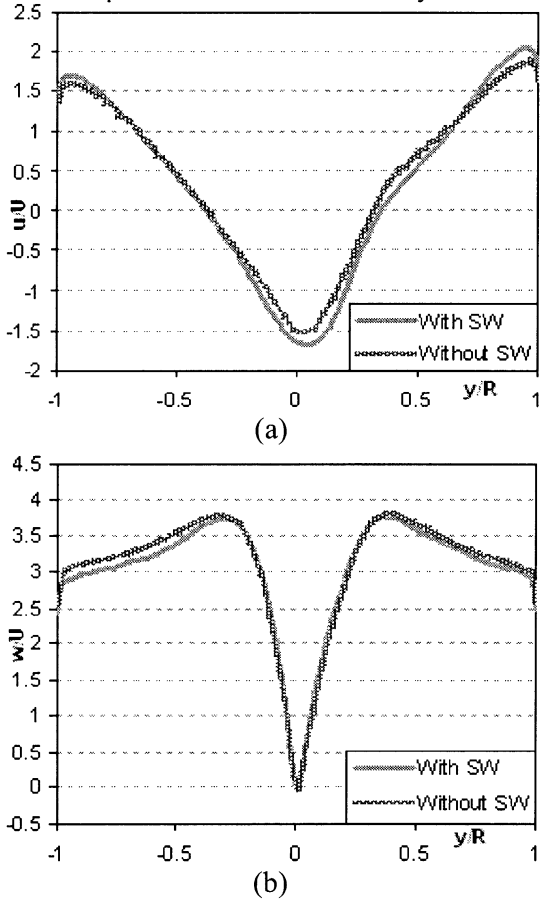

Figure 11
Time-averaged velocity profiles with and without swirler along a line at x/L=0.4:
a: axial velocity, b: circumferential velocity

the recirculation zone compared to 3D URANS RSM (Figure 12a). Comparing the time-averaged circumferential velocity profiles, one can observe that 3D URANS RSM predicts a more confined vortex core with substantially higher velocities compared to 3D URANS SST. For the comparison of time-averaged axial and circumferential velocities by 3D URANS RSM and 3D URANS SST, similar trends are observed, also for x/L=0.4. The 2D RANS SST results predict an even larger recirculation zone and a broader vortex core (with smaller maximum velocities) compared to 3D URANS SST. It is already mentioned above that no convergence could be obtained by 2D RANS RSM, which can be seen as the manifestation of the ability of RSM to capture low frequency flow unsteadiness. The 2D URANS RSM results displayed in the figures predict a qualitatively complete different axial velocity field,

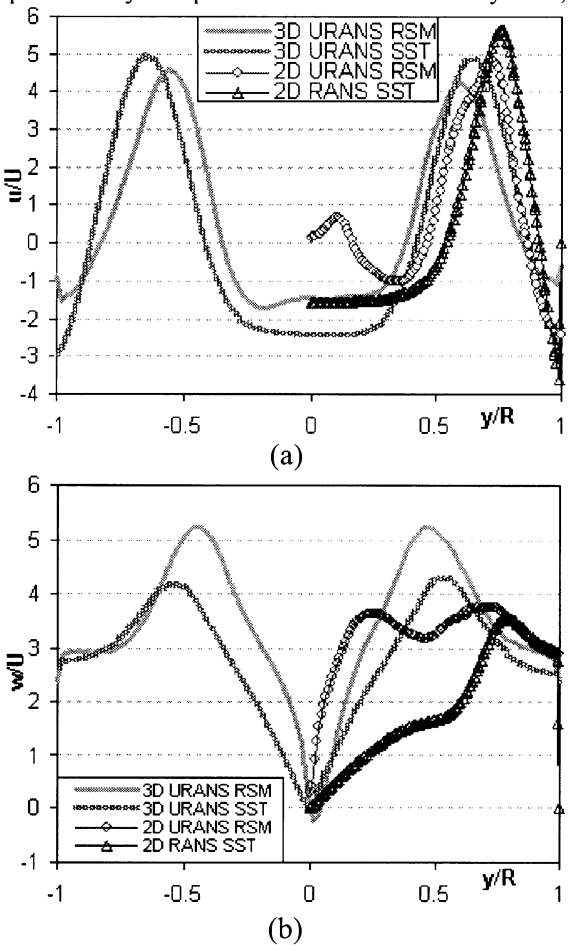

Figure 12
Time-averaged velocity profiles for different turbulence models along a line at x/L=0.2:
a: axial velocity, b: circumferential velocity

implying a region of forward flow (central jet) enveloped by a recirculation zone. The circumferential velocity profiles of 2D URANS RSM also differ considerably from those of 3D URANS RSM. This comparison shows the importance of three-dimensional effects combined with flow unsteadiness.

CONCLUSIONS

Turbulent swirling flow in water model of a gas turbine combustor is computationally investigated. As the basic modeling strategy, a 3D unsteady RANS (URANS) approach is applied, employing a differential Reynolds stress turbulence model (RSM). A highly unsteady and three-dimensional

flow structure, exhibiting vortex breakdown and a precessing vortex core are observed.

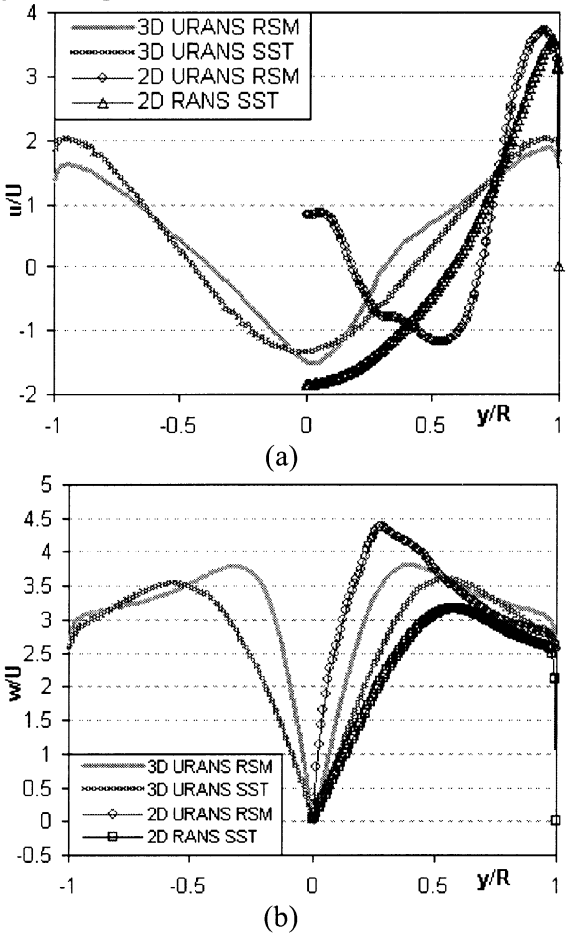

Figure 13
Time-averaged velocity profiles for different turbulence models along a line at x/L=0.4:
a: axial velocity, b: circumferential velocity

For better understanding their influence, computations are carried out for different modeling parameters. Main findings can be summarized as:

- For obtaining a sufficiently stationary time-averaged flow field, the time-averaging time should be about 7 times the integral time scale.
- The time-averaged results don't get effected by the time-step size, for time-step sizes resulting in maximum cell Courant numbers up to four.
- An omission of the swirler results in a smaller size and intensity of the inner recirculation zone near the inlet. In farther downstream positions, differences between the cases die out.
- Differences between 3D URANS RSM and 3D URANS SST are rather substantial. The larger differences are observed for the time-averaged circumferential velocity profile, as the former predicts a more intense vortex core with higher maximum velocities. 2D RANS SST results may only be used for purely qualitative purposes. 2D RANS RSM did not lead to converged results. 2D URANS RSM leads to substantially different results compared to 3D URANS RSM.

ACKNOWLEDGEMENTS

We would like to thank the management board of MAN Turbo AG for the permission to publish this paper.

REFERENCES

1. Benim, A. C. (1990): Finite element Analysis of confined swirling flows, Int. J. Numer. Methods Fluids, Vol. 11, pp. 697-717.
2. Escudier, M. and Keller, J. J. (1983): Vortex breakdown: a two-stage transition, aerodynamics of vortical type flows in three-dimensions, AGARD CP No. 342, Paper No. 25.
3. Launder, B. E., Reece, G. J. and Rodi, W. (1975): Progress in the development of a Reynolds-stress turbulence closure, J. Fluid Mechanics, Vol. 68, pp. 537-566.
4. Speziale, C.G., Sarkar S., Gatski, T.B. (1991): Modelling the pressure-strain correlation of turbulence, J. Fluid Mech.,V.227,pp.245-272.
5. Benim, A. C. and Nahavandi, A. (2003): A computational analysis of turbulent swirling flows, in: Hanjalic, K., Nagano,Y. and Tummers, M. J. (Eds.), Turbulence, Heat and Mass Transfer 4, Begell House, New York,pp.715-722.
6. Benim, A. C., Nahavandi, A. and Syed, K. J. (2005): URANS and LES analysis of turbulent swirling flows, Prog. Comput. Fluid Dynamics, Vol. 5 pp. 444-454.
7. Benim A. C., Escudier, M. P., Nahavandi, A., Nickson, K. and Syed . K. J. (2008): "DES analysis of confined turbulent swirling flows in the sub-crirtical regime, in Peng, S. H.,Haase,W. (Eds.) Advances in Hybrid RANS-LES Modelling, Springer, Berlin, pp.172-181.
8. Benim, A. C., Escudier, M. P., Nahavandi, A., Nickson, K. amd Syed, K. J. (2008): Experimental and Numerical Investigation of Incompressible Turbulet Flow in an Idealized Swirl Combustor", International Journal of Heat and Fluid Flow (submitted).
9. ANSYS-CFX-11 Solver Manual (2008).
10. Hunt, J. C. R., Wray, A. A. and Moin, P. (1988): Eddies, stream and convergence zones in

turbulent flows, Report CTR-S88, Stanford U.